Supporting Information

Sublimation-induced gas-reacting process for high energy density Ni-rich electrode materials

Jieun Kim, [a] Junghwa Lee, [a] Changgeun Bae [a] and Byoungwoo Kang *[a]

[a]Department of Materials Science and Engineering, Pohang University of Science and Technology (POSTECH), 77 Cheongamro, Nam-Gu, Pohang 37673, Republic of Korea.

* Corresponding author
E-mail address: bwkang@postech.ac.kr

Table S1. Summary of reported surface modification processes and the SIGR process (This work) for $LiNi_xCo_yMn_{1-x-y}O_2$ and $LiNi_xCo_yAl_{1-x-y}O_2$ ($0.7 \leq x \leq 0.9$) electrode materials in terms of their process, electrochemical condition, and performance.

Cathode	Surface modification process		Electrochemical condition	Electrochemical performance
	Method	Temperature	Voltage range	Retention of bare/modified sample – improved retention compared to bare (cycle)
This work (Li-S-O coated $LiNi_{0.8}Co_{0.1}Mn_{0.1}O_2$)	**Dry mixing by hand & annealing**	**300℃**	**2.5-4.5V**	**89.8% / 96.2% – 6.4% (50)** **83.4% / 92.0% – 8.6% (100)** **74.5% / 88.9% – 14.4% (150)** **70.1% / 83.8% – 13.7% (200)**
Li_3PO_4 coated $LiNi_{0.76}Co_{0.1}Mn_{0.14}O_2$[1]	ALD & annealing	600℃	2.7-4.5V	79.0% / 91.6% – 12.6% (200)
PEDOT coated $LiNi_{0.85}Co_{0.1}Mn_{0.05}O_2$[2]	oCVD	90℃	2.7-4.3V	54% / 91% – 37% (100)
Concentration gradient $LiNi_{0.865}Co_{0.12}Al_{0.015}O_2$[3]	Coprecipitation	680℃	2.7-4.3V	84.6% / 91.6% – 7.0% (100)
Li_3PO_4 coated $LiNi_{0.84}Co_{0.14}Al_{0.02}O_2$[4]	Prepitation reaction & mixing for 1h & annealing	700℃	2.8-4.4V	80% / 91% – 11% (50)
$LiZr_2(PO_4)_3$ coated $LiNi_{0.82}Co_{0.15}Al_{0.03}O_2$[5]	Mixing in ethanol & annealing	750℃	2.7-4.3V	69.4% / 84.6% – 15.2% (100)
Li_3PO_4, graphene coated $LiNi_{0.8}Co_{0.1}Mn_{0.1}O_2$[6]	Stirring at 500rpm & annealing	500℃	3.0-4.3V	88.1% / 94.3% – 6.2% (150)
Li_2TiO_3 coated $LiNi_{0.8}Co_{0.15}Al_{0.05}O_2$[7]	Synthesizing Li_2TiO_3 & stirring & annealing	700℃/600℃	3.0-4.3V	93.42% / 96.69% – 3.27% (100)
Li-Zr-O coated $LiNi_{0.8}Co_{0.1}Mn_{0.1}O_2$[8]	Stirring for 2h & annealing	400℃	3.0-4.3V	91.1% / 94.3% – 3.2% (50)
Co-related materials coated $LiNi_{0.8}Co_{0.1}Mn_{0.1}O_2$[9]	Mixing at 1500rpm & annealing	750℃	3.0-4.3V	– 5% (200)

Table S2. Summary of reported surface modification processes and the SIGR process (This work) for $LiNi_xMe_yO_2$ ($0.9 \leq x \leq 1$, Me = metals) electrode materials in terums of their process, electrochemical condition, and performance.

Cathode	Modification process		Electrochemical condition	Electrochemical performance
	Method	Temperature	Voltage range	Retention of bare/modified sample - improved retention compared to bare (cycle)
This work (Li-S-O coated $LiNiO_2$)	**Dry mixing by hand & annealing (coating)**	**300℃**	**2.5-4.5V**	**70.8% / 92.0% – 21.2% (50)** **62.1% / 84.8% – 22.7% (100)** **54.7% / 80.2% – 25.5% (150)** **53.2% / 76.8% – 23.6% (200)**
$LiNi_{0.9}W_{0.1}O_2$[10]	Doping		2.7-4.3V	73.7% / 90.3% – 16.6% (100)
$C_4H_6CoO_4$ coated $LiNiO_2$[11]	Stirring in ethanol & annealing (coating)	500℃	3.0-4.2V	76.4% / 87.4% – 11.0% (50)
$Li_{0.98}Mg_{0.02}Ni_{0.0.94}Co_{0.06}O_2$[12]	Doping		2.8-4.4V	77% / 90% – 13% (150)
$LiNi_{0.9}Co_{0.05}Mn_{0.05}O_2$ with concentration gradient shell[13]	Concentration gradient coating (coprecipitation)		2.8-4.4V	85.2% / 92.2% – 7% (100)
$LiNi_{0.94}Zr_{0.04}O_2$[14]	Doping		2.7-4.3V	81% / 74% – 7% (100)

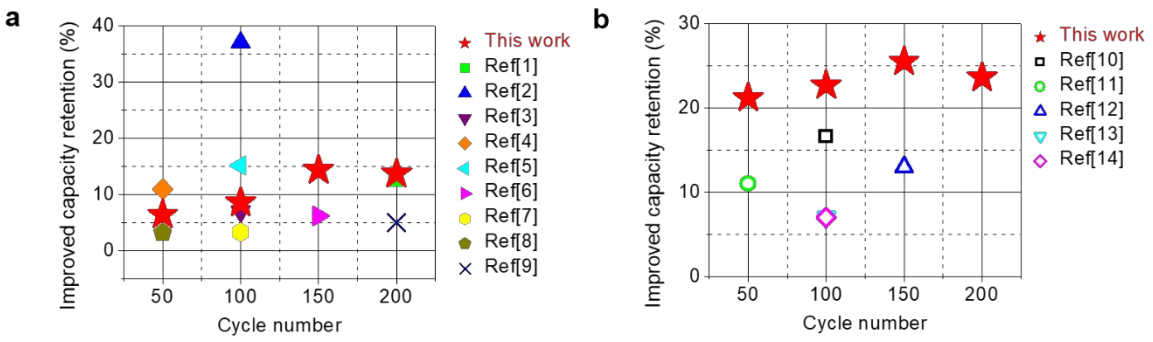

Figure S1. Comparison of the improvments in the dicharge capacity retention with other reported results **(a)** SNCM and **(b)** SLNO sample with other recent papers.

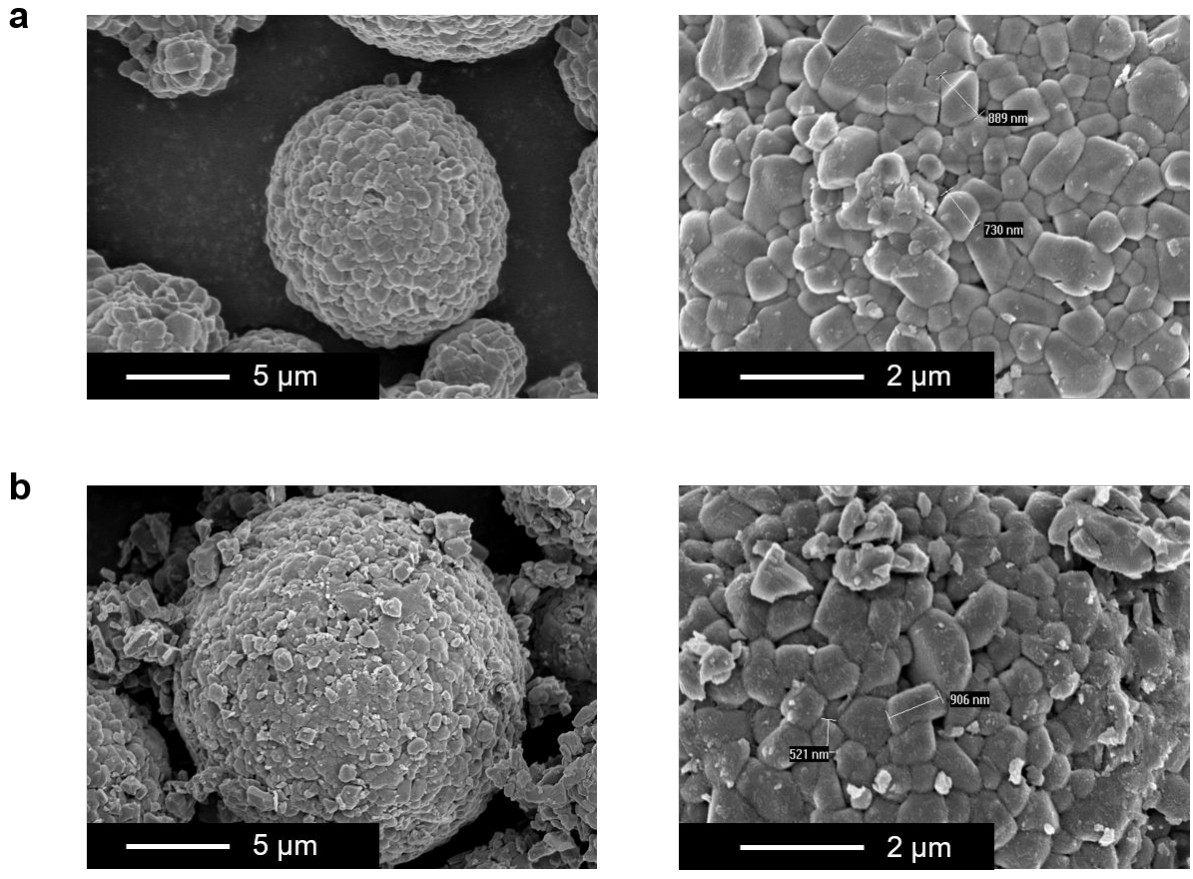

Figure S2. Scanning electron microscopy (SEM) images of the **(a)** NCM sample and **(b)** SNCM sample.

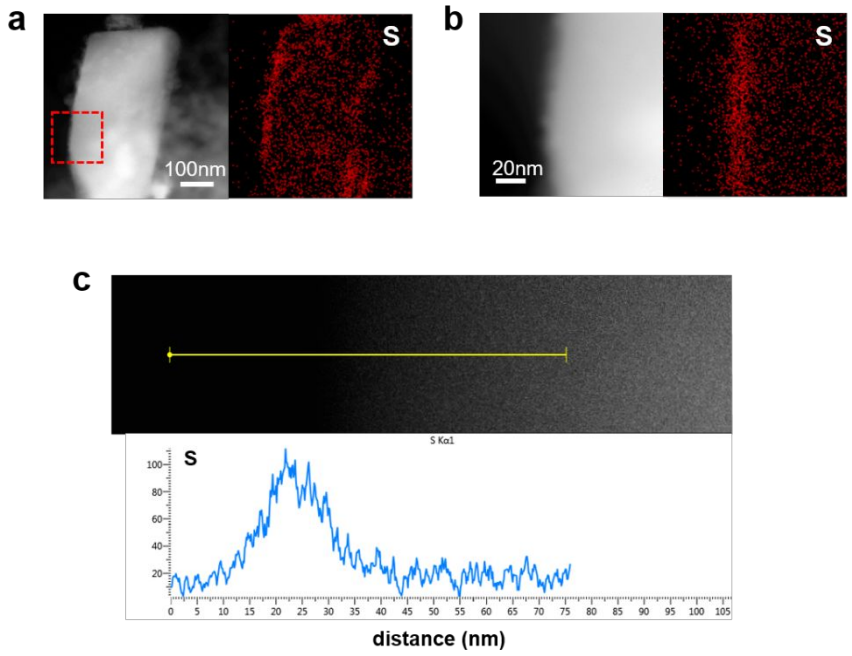

Figure S3. (a) STEM-HAADF image and EDS mapping results of the primary particle of the SNCM sample. **(b)** Magnified image of the red box in (a). **(c)** EDS line mapping of the surface in (b).

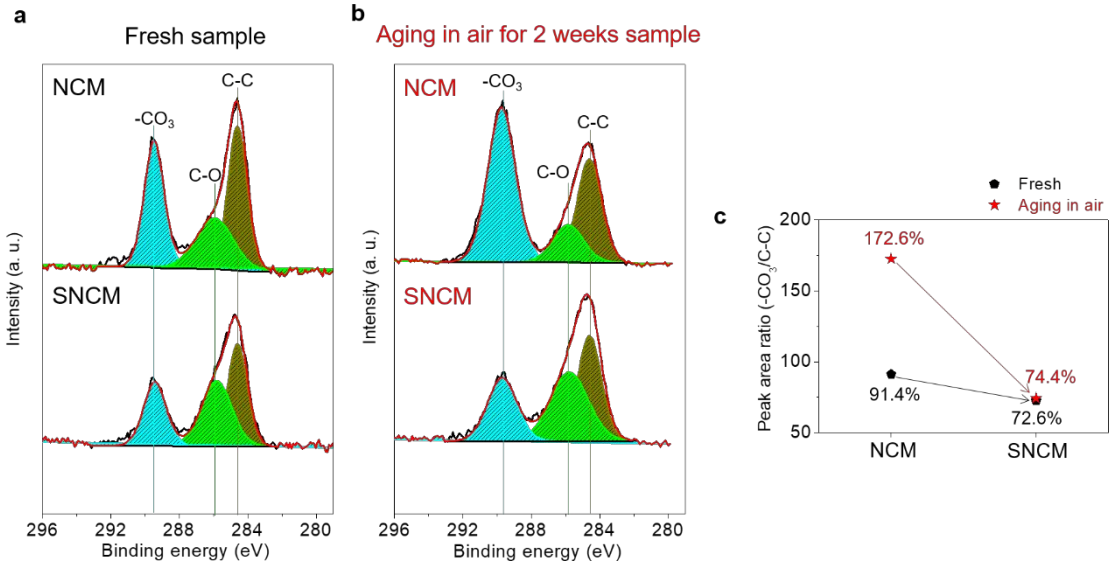

Figure S4. XPS spectra of the C 1s of **(a)** fresh NCM and SNCM and **(b)** NCM after aging in air for 2 weeks and sublime-induced gas reacting process using the NCM sample after aging in air for 2 weeks. **(c)** Area ratio of $-CO_3$ peak to C-C peak of the NCM and SNCM.

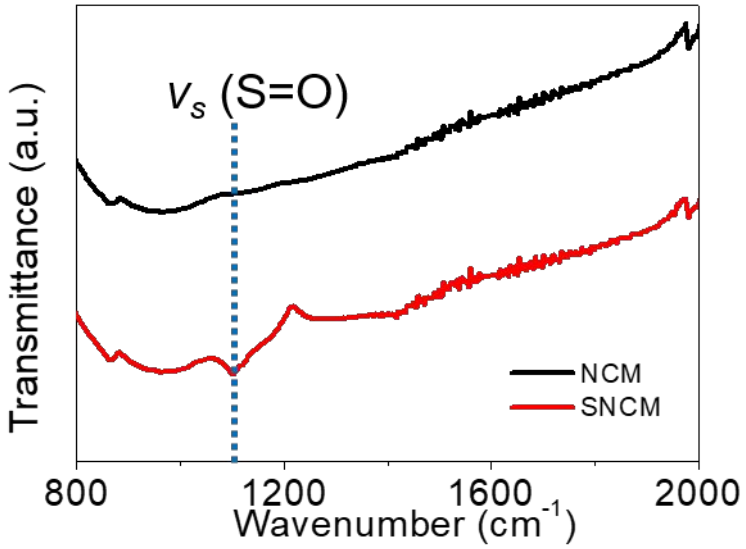

Figure S5. ATR-FTIR spectra of the NCM and SNCM, revealing that the SNCM sample can have the S=O bonding environment.[15]

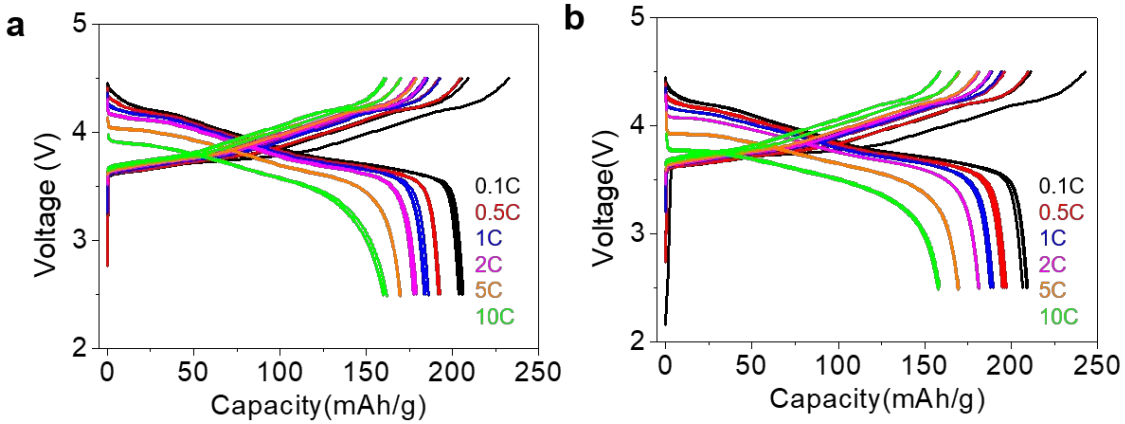

Figure S6. Voltage profiles in discharge rate capability test of **(a)** the NCM and **(b)** SNCM.

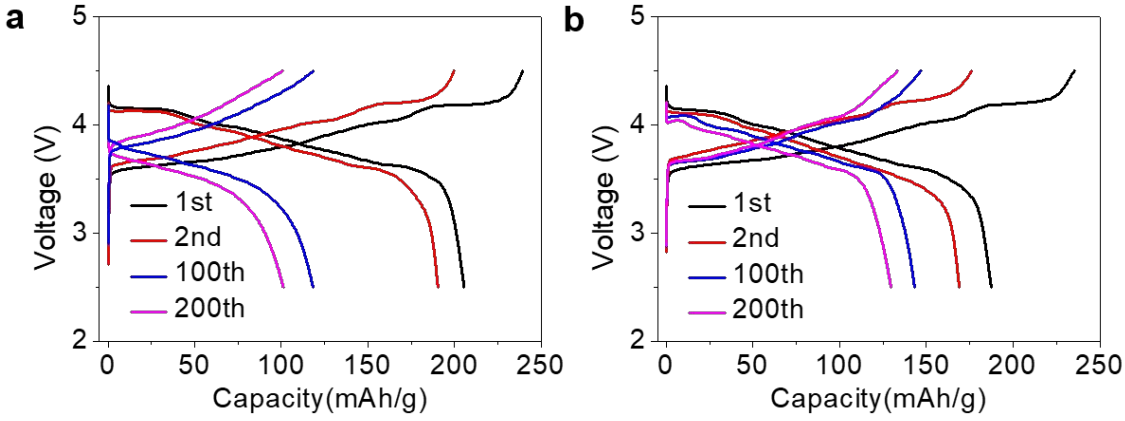

Figure S7. Voltage profiles of **(a)** LNO and **(b)** SLNO in the voltage range 2.5V-4.5V at room temperature. The half-cell is cycled at C/3 after first cycle at C/10, where 1C corresponds to the current density of 200mA/g.

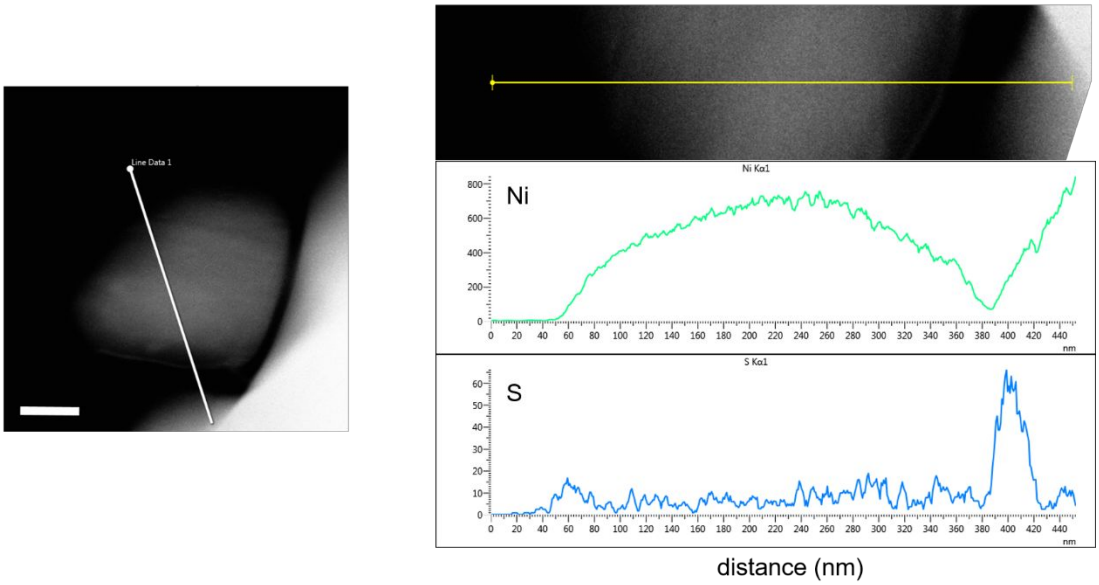

Figure S8. STEM-HAADF image and EDS line mapping of the SNCM after 50 cycles. Scale bar, 100nm.

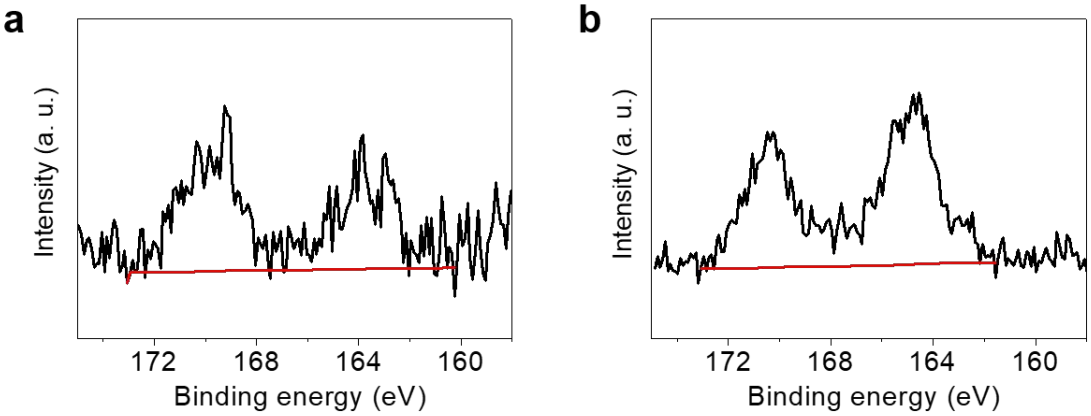

Figure S9. XPS data of the S 2p of the SNCM electrode **(a)** before cycling and **(b)** after 200 cycles.

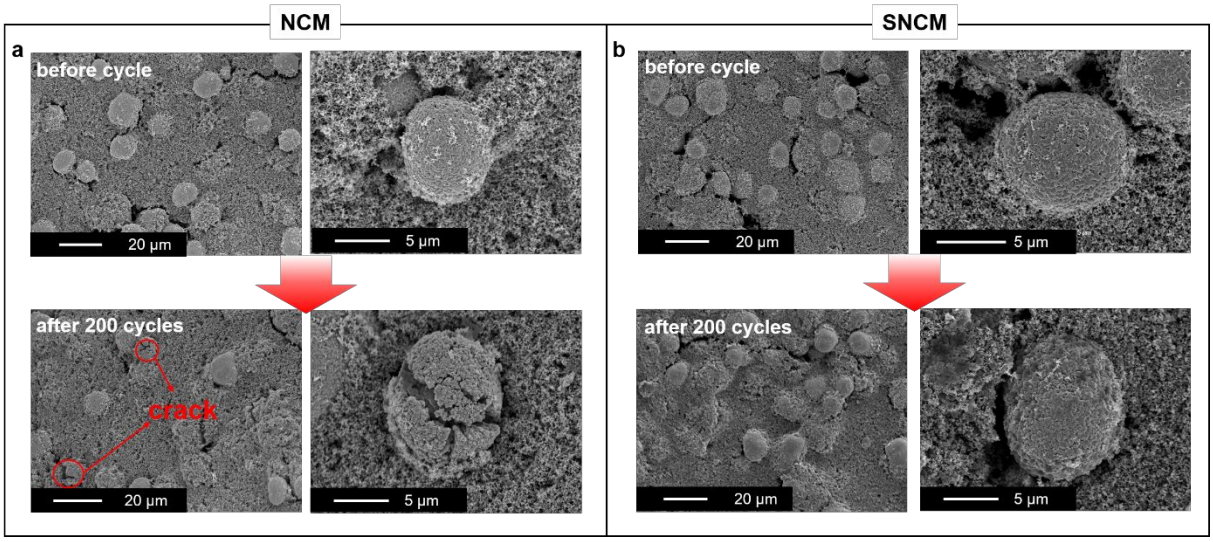

Figure S10. SEM images of the electrodes before/after cycles **(a)** NCM electrode and **(b)** SNCM electrode.

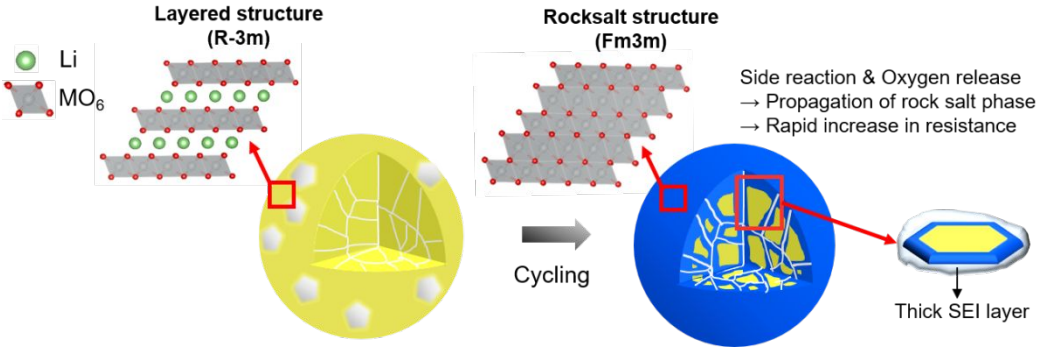

Figure S11. Schematic showing the structural changes on cycling of the NCM.

Table S3. pH value of the NCM and SNCM.

	NCM	**SNCM**
pH value	10.6	9.9

Reference

(1) Yan, P. F.; Zheng, J. M.; Liu, J.; Wang, B. Q.; Cheng, X. P.; Zhang, Y. F.; Sun, X. L.; Wang, C. M.; Zhang, J. G. Tailoring Grain Boundary Structures and Chemistry of Ni-Rich Layered Cathodes for Enhanced Cycle Stability of Lithium-Ion Batteries. *Nat Energy* **2018,** *3* (7), 600-605.

(2) Xu, G. L.; Liu, Q.; Lau, K. K. S.; Liu, Y.; Liu, X.; Gao, H.; Zhou, X. W.; Zhuang, M. H.; Ren, Y.; Li, J. D.; Shao, M. H.; Ouyang, M. G.; Pan, F.; Chen, Z. H.; Amine, K.; Chen, G. H. Building Ultraconformal Protective Layers on Both Secondary and Primary Particles of Layered Lithium Transition Metal Oxide Cathodes. *Nat Energy* **2019,** *4* (6), 484-494.

(3) Park, K. J.; Choi, M. J.; Maglia, F.; Kim, S. J.; Kim, K. H.; Yoon, C. S.; Sun, Y. K. High-Capacity Concentration Gradient Li[Ni0.865Co0.120Al0.015]O-2 Cathode for Lithium-Ion Batteries. *Adv Energy Mater* **2018,** *8* (19).

(4) Kim, J.; Lee, J.; Ma, H.; Jeong, H. Y.; Cha, H.; Lee, H.; Yoo, Y.; Park, M.; Cho, J. Controllable Solid Electrolyte Interphase in Nickel-Rich Cathodes by an Electrochemical Rearrangement for Stable Lithium-Ion Batteries. *Adv Mater* **2018,** *30* (5).

(5) Zhang, J. F.; Zhang, J. Y.; Ou, X.; Wang, C. H.; Peng, C. L.; Zhang, B. Enhancing High-Voltage Performance of Ni-Rich Cathode by Surface Modification of Self-Assembled Nasicon Fast Ionic Conductor LiZr2(PO4)(3). *Acs Appl Mater Inter* **2019,** *11* (17), 15507-15516.

(6) Fan, Q. L.; Yang, S. D.; Liu, J.; Liu, H. D.; Lin, K. J.; Liu, R.; Hong, C. Y.; Liu, L. Y.; Chen, Y.; An, K.; Liu, P.; Shi, Z. C.; Yang, Y. Mixed-Conducting Interlayer Boosting the Electrochemical Performance of Ni-Rich Layered Oxide Cathode Materials for Lithium Ion Batteries. *J Power Sources* **2019,** *421*, 91-99.

(7) He, X. S.; Xu, X.; Wang, L. G.; Du, C. Y.; Cheng, X. Q.; Zuo, P. J.; Ma, Y. L.; Yin, G. P. Enhanced Electrochemical Performance of LiNi0.8Co0.15Al0.05O2 Cathode Material Via Li2TiO3 Nanoparticles Coating. *J Electrochem Soc* **2019,** *166* (2), A143-A150.

(8) Lim, Y. J.; Lee, S. M.; Lim, H.; Moon, B.; Han, K. S.; Kim, J. H.; Song, J. H.; Yu, J. S.; Cho, W.; Park, M. S. Amorphous Li-Zr-O Layer Coating on the Surface of High-Ni Cathode Materials for Lithium Ion Batteries. *Electrochim Acta* **2018,** *282*, 311-316.

(9) Kim, J.; Ma, H.; Cha, H.; Lee, H.; Sung, J.; Seo, M.; Oh, P.; Park, M.; Cho, J. A Highly Stabilized Nickel-Rich Cathode Material by Nanoscale Epitaxy Control for High-Energy Lithium-Ion Batteries. *Energ Environ Sci* **2018,** *11* (6), 1449-1459.

(10) Ryu, H. H.; Park, G. T.; Yoon, C. S.; Sun, Y. K. Suppressing Detrimental Phase Transitions Via Tungsten Doping of LiNiO2 Cathode for Next-Generation Lithium-Ion Batteries. *J Mater Chem A* **2019,** *7* (31), 18580-18588.

(11) Li, Y. J.; Deng, S. Y.; Chen, Y. X.; Gao, J.; Zhu, J.; Xue, L. L.; Lei, T. X.; Cao, G. L.; Guo, J.; Wang, S. L. Dual Functions of Residue Li-Reactive Coating with C4H6COO4 on High-Performance LiNiO2 Cathode Material. *Electrochim Acta* **2019,** *300*, 26-35.

(12) Xie, Q.; Li, W. D.; Manthiram, A. A Mg-Doped High-Nickel Layered Oxide Cathode Enabling Safer, High-Energy-Density Li-Ion Batteries. *Chem Mater* **2019,** *31* (3), 938-946.

(13) Kim, U. H.; Ryu, H. H.; Kim, J. H.; Mucke, R.; Kaghazchi, P.; Yoon, C. S.; Sun, Y. K. Microstructure-Controlled Ni-Rich Cathode Material by Microscale Compositional Partition for Next-Generation Electric Vehicles. *Adv Energy Mater* **2019,** *9* (15).

(14) Yoon, C. S.; Choi, M. J.; Jun, D. W.; Zhang, Q.; Kaghazchi, P.; Kim, K. H.; Sun, Y. K. Cation Ordering of Zr-Doped LiNiO2 Cathode for Lithium-Ion Batteries. *Chem Mater* **2018,** *30* (5), 1808-1814.

(15) Diao, Y.; Xie, K.; Xiong, S. Z.; Hong, X. B. Insights into Li-S Battery Cathode Capacity Fading Mechanisms: Irreversible Oxidation of Active Mass During Cycling. *J Electrochem Soc* **2012,** *159* (11), A1816-A1821.